# Ionic Technologies Inc.

*For Additional Information send inquiries to sales@ionic-tech.com or call at 864-288-9111*

Industrial Heating
Magazine Articles

## Plasma Nitriding of Stainless Steels

*by Luiz Carlos Casteletti*
*Amadeu Lombardi Neto*
*G.E. Totten*
*March 5, 2008*

*Stainless steels are widely used in the chemical, petrochemical and food-processing industries due to their favorable corrosion properties. The industrial world would not exist without this class of material.[1] They exhibit generally poor tribological properties, however, which limit their applications to use in tribocorrosive environments.*

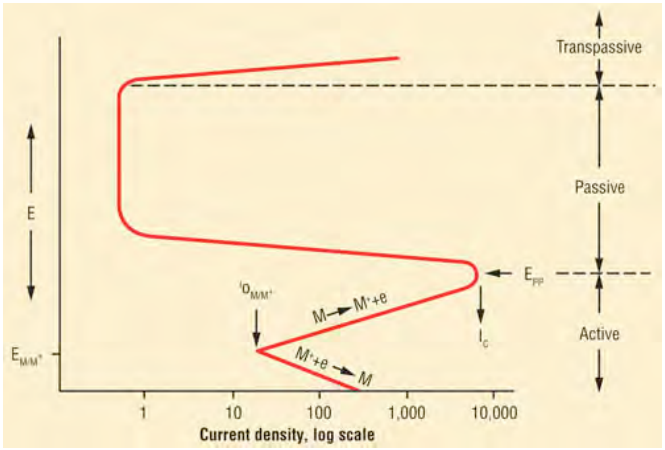

Fig. 1. Typical anodic-dissolution behavior of an active-passive metal

Surface treatments such as nitriding can enhance the surface hardness of these steels, which improves wear resistance.[2-11] Gas nitriding with ammonia produces a surface layer that consists of a mixture of Fe4N and Fe2-3N nitrides, which are due to the variability of ammonia dissociation (nitriding potential) as the layer is formed. In conventional gas nitriding, the nascent (elemental) nitrogen is produced by introducing ammonia (NH3) to a heated (>480°C, 900°F) work surface.

The nitriding potential, which determines the rate of introduction of nitrogen to the surface, is determined by the NH3 concentration at the work surface and its rate of dissociation. The nitriding potential can vary significantly in the conventional gas process and is responsible for the limited control of the microstructure in the nitrided layer. X-ray diffraction has shown that from the outer surface to the beginning of the diffusion layer the dominant phase changes from Fe2-3N to Fe4N. However, both phases exist throughout the entire diffusion layer, and it is therefore referred to as a "dual-phase layer." The nitride layers are called the "white layer" because they are not etched by metallographic reagents.[2-3]

The dual-phase layer has two characteristics that make it susceptible to fracture. The first is that the different crystalline structures exhibit weak bonding at the interface between phases, and the second is the different thermal-expansion coefficients of the two phases. Layers that are particularly thick or that are subjected to temperature fluctuation in service are particularly prone to failure. Another mechanical weakness in the gas-nitrided layer is porosity in the outer region of the layer. As it increases in thickness, ammonia dissociation becomes slower due to reduced catalytic action of the steel surface and gas bubbles begin to form in the layer.[2-3]

## Plasma Nitriding

**Table 1. Chemical compositions of the steels (wt%)**

| | C (%) | Cr(%) | Ni(%) | Mo(%) | Mn(%) | Si(%) | N(%) | Cu(%) | Fe(%) |
|---|---|---|---|---|---|---|---|---|---|
| **316L** | 0.028 | 17.06 | 10.48 | 2.44 | 1.49 | 0.53 | - | - | Bal. |
| **409** | 0.030 | 11.25 | 0.06 | 0.11 | 0.74 | 0.49 | - | - | Bal. |
| **Super-Duplex** | 0.023 | 24.81 | 7.52 | 4.05 | 0.62 | - | 0.30 | 0.176 | Bal. |

Plasma nitriding is a method of surface hardening using glow-discharge technology to introduce nascent (elemental) nitrogen to the surface of a metal part for subsequent diffusion into the material. In a vacuum, high-voltage electrical energy is used to form a plasma through which nitrogen ions are accelerated to impinge on the workpiece. This ion bombardment heats the workpiece and cleans the surface providing active nitrogen. A key difference between gas and ion nitriding is the mechanism used to generate nitrogen at the surface of the work.

In the plasma-nitriding process, nitrogen gas (N2) can be used instead of ammonia because the gas is dissociated to form elemental nitrogen under the influence of the glow discharge. Therefore, the nitriding potential can be precisely controlled by the regulation of the N2 content in the process gas. This control allows precise determination of the composition of the entire nitrided case, selection of a monophase layer of Fe2-3N or Fe4N or total prevention of white-layer formation.

## Advantages

Plasma nitriding exhibits a strong advantage relative to the conventional gas process for nitriding stainless steels. The chromium-oxide passive layer on the surface of these materials represents a barrier to nitriding and must be removed prior to nitriding. With conventional gas nitriding, several cleaning processes – wet blasting, pickling and chemical reduction – have been developed to remove the oxide. With ion nitriding, however, this passive layer can be removed by sputtering with hydrogen in the vessel itself just prior to introducing the process gas.

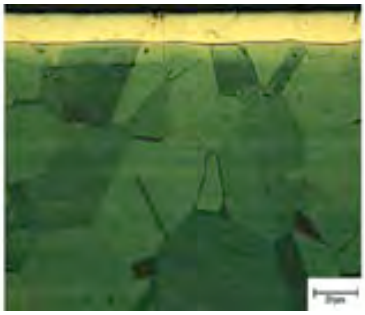

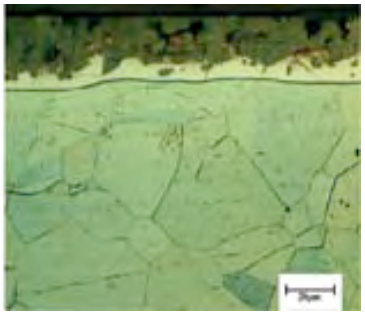

Fig. 2. AISI 316L nitrided at 400□C (752□F); Fig. 3. AISI 316L nitrided at 450□C (842□F); Fig. 4. AISI 316L nitrided at 500□C (932□F)

Plasma nitriding exhibits a number of the following additional advantages.

- Metallurgical control of the process is much simpler than with conventional gas processes. Case formation can be either single-phase, dual-phase or diffusion zone only.
- Improved control of case thickness.
- The process is conducted at a lower temperature due to plasma activation.
- Plasma nitriding typically exhibits lower distortion.
- Reduced treatment times for plasma nitriding. There is no environmental hazard since no ammonia is involved – the process gas is a mixture of H2 and N2.[2, 3]

Thermochemical plasma treatments are a very adequate way to improve stainless steels. Plasma nitriding can be carried out at temperatures from 350-500˚C (662-932□F). While giving significant improvement in wear resistance, the higher treatment temperatures tend to adversely affect the corrosion performance of the stainless steels due to the formation of CrN. This same phenomenon occurs with gas nitriding, which requires higher treatment temperatures.[2, 3]

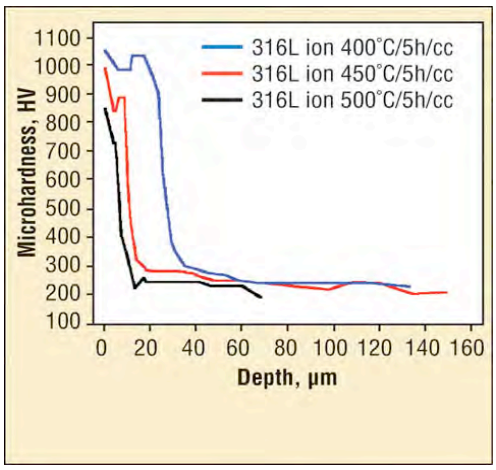

Fig. 5. Nitrided AISI 316L stainless steel micro-hardness curves

Plasma-nitriding treatments typically result in the formation of a layer of austenite that is supersaturated with respect to nitrogen called "expanded austenite" or "S phase." The S phase can exhibit hardness of up to four times greater than the substrate, which enhances the wear resistance without compromising the improved corrosion resistance.[4-16]

Figure 1 illustrates a typical S-shaped dissolution curve for a passive metal or alloy. A decrease in the dissolution rate accompanying the active-to-passive transition is shown. This decrease in dissolution rate occurs just above the primary passive potential (Epp) and is the result of protective-film formation at this point. One of the important characteristics of an active-passive metal is the position of its anodic current-density maximum, which is characterized by the Epp and the critical anodic current density for passivity (Ic). The greater the Ic, the greater the corrosion rate of the material. Therefore, the dislocation of the curve to the right indicates increased corrosion of the material.[17]

Martensitic, ferritic and austenitic-ferritic stainless steels can all be treated by plasma nitriding to obtain a layer similar to those produced with austenitic stainless steels, which is composed of an S phase that increases hardness and wear resistance.

## Experimental

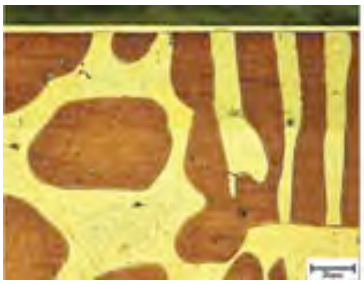
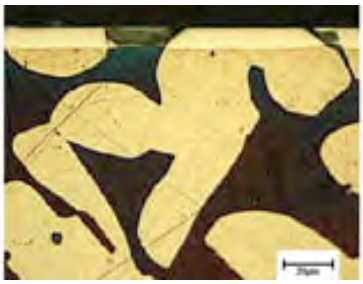
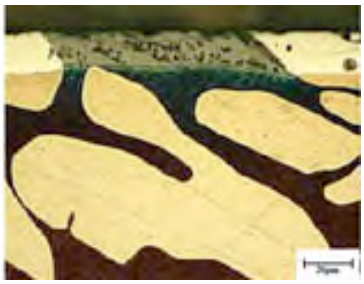

Fig. 6. Duplex stainless steel nitrided at 400☒C (752☒F); Fig. 7. Duplex stainless steel nitrided at 450☒C (842☒F); Fig. 8. Duplex stainless steel nitrided at 500☒C (932☒F)

The alloys used for the plasma-nitriding treatments are: AISI 316L austenitic stainless steel, AISI 409 ferritic stainless steel and ASTM Super-duplex A890 Gr5A steel – all in the solubilized conditions. The solubilization temperature was 1050°C (1922°F) for 30 minutes with cooling in water. Table 1 presents the nominal chemical compositions of the steels used in this work.

Cylindrical test specimens were machined with 12mm diameter and 3mm thickness. Their surfaces were ground using sandpaper and polished with 0.05mm alumina.

The plasma-nitriding treatments were conducted using direct current. For the nitriding treatments, a gaseous mixture of 20% H2-80% N2 at an 8x10-2 mbar pressure was used. The nitriding temperatures were 400☒C (752˚F), 450☒C (842˚F) and 500☒C (932˚F) for a time of five hours. The samples were cooled inside the vacuum chamber.

Metallographic and microhardness analyses were performed after the plasma-nitriding treatment. The reagents Nitromuriatic and Beraha II were used for the metallographic etching of the samples.

Wear tests were performed with calotest-type equipment using a 75N load without abrasives. Each sample was tested for 50 minutes, and at 5, 10 and 15 minutes the test was stopped, and the diameter of the caps produced were measured to determine the wear volume.

Corrosion tests of the potentiodynamic type of the treated samples were performed using a desaerated NaCl solution in water (3.5%) with neutral pH at 25°C, according the ASTM G61 Standard.

X-ray diffraction analyses were conducted on the nitrided samples and on their substrates for phase identification.

## Results

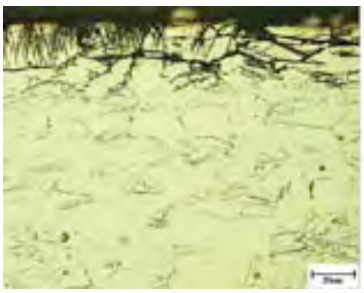
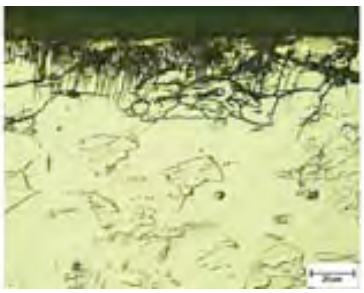
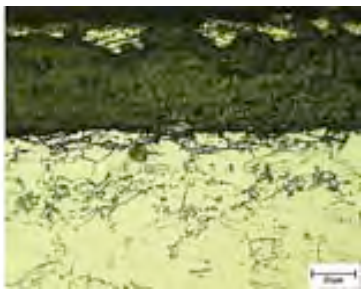

Fig. 10. AISI 409 stainless steel nitrided at 400☒C (752☒F); Fig. 11. AISI 409 stainless steel nitrided at 450☒C (842☒F); Fig. 12. AISI 409 stainless steel nitrided at 500☒C (932☒F)

### Micrographic Analysis and Microhardness of the Layers

Figures 2, 3 and 4 show the optical micrographs, and Figure 5 shows the microhardnesses obtained for the nitrided layers formed after the specified nitriding treatment for 316L. The austenitic substrate and

the nitrided layers vary with increasing treatment temperature. In the samples nitrided at 400°C and 450°C, a single phase called "S" or "expanded austenite" phase was formed while the sample nitrided at 500°C resulted in the formation of a dark layer of chrome nitrides over the S phase.

Figure 5 shows the microhardness profiles of the cross section of the nitrided layers. In all cases, the effectiveness of the treatments to increase the surface hardness of the steel was verified. It was seen that the nitriding temperature influences the hardness of the layers. The nitrided layer obtained at 500°C had a higher microhardness value and a greater depth due to the presence of chrome nitrides and the high concentration of nitrogen in the white layer (S phase).

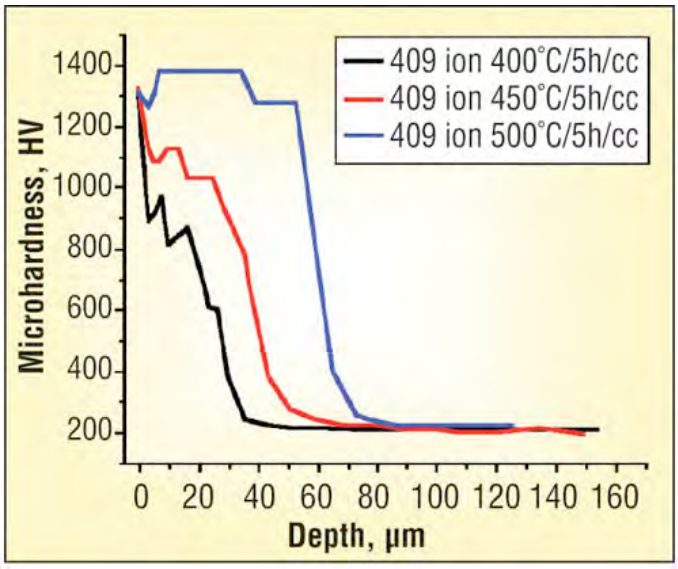


Fig. 13. Nitrided AISI 409 stainless steel microhardness curves

Similarly, Figures 6-9 show the effects of treating the duplex stainless. These figures show the austenitic/ferritic substrate and nitrided surface. Figure 9 shows that the sample nitrided at 500□C exhibited the highest surface hardness due to the higher nitrogen concentration in the S phase.

Figures 10-13 show the effects of treating AISI 409 stainless steel. These micrographs demonstrate the growth of an acicular phase, which is probably iron nitrides. For the treatment conducted at 500□C, the formation of a dark phase consisting of chromium nitrides was observed. Figure 13 shows that the surface hardnesses of the nitrided samples are increased by a factor of 5-6 times relative to the ferritic-matrix hardness.

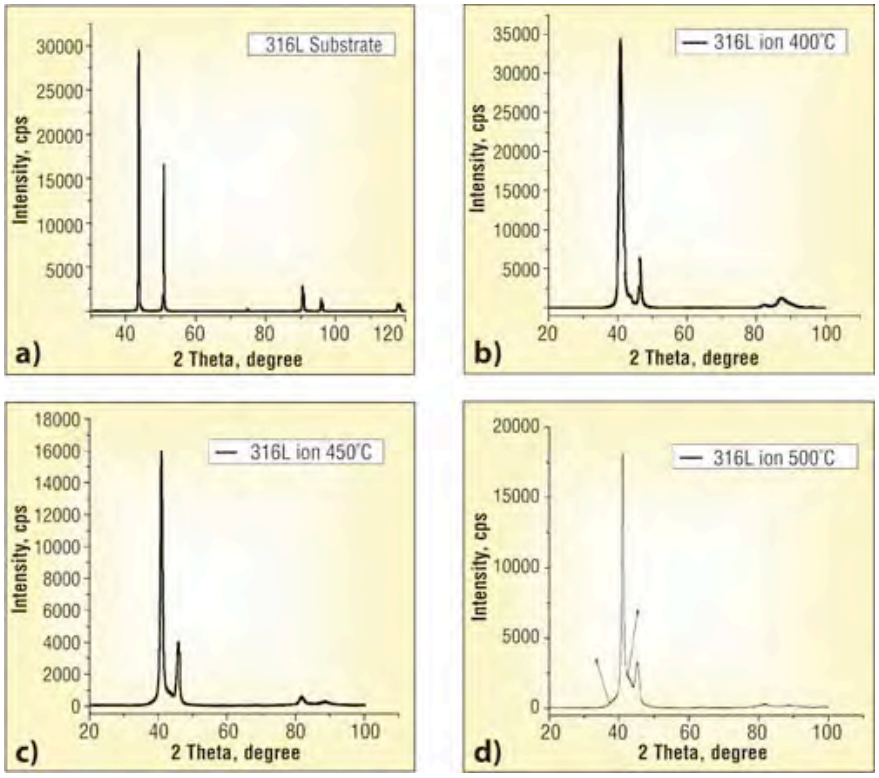


Fig. 14. X-ray diffraction patterns of the AISI 316L steel: (a) substrate; (b) 400□C; (c) 450□C; (d) 500□C all for five hours

## X-ray Diffraction Analysis

Figure 14 illustrates the X-ray diffraction patterns obtained for the nitrided layers produced on the AISI 316L stainless steel. Figure 14a indicates the presence of the standard austenite peaks corresponding to the face-centered body matrix. The wider peaks shown in the diffraction patterns of Figures 14b and 14c indicate the presence of S phase. This expanded austenite phase can contain up to 42% nitrogen at the surface. It also improves the corrosion resistance of the base stainless steel. Within a few micrometers from the surface, however, the nitrogen content decreases to about 20-35 atomic%. Hardness of the S phase coatings achieve maximum value of HV=2000 at 28-32 at% nitrogen.[4-16] Figure 14d illustrates the presence of expanded austenite and chromium nitrides. The development of high residual-compressive stresses in the nitrided layer obtained at low temperatures may be responsible for the displacement of the diffraction-peak positions observed.

## Wear Tests

Figures 15a to 17a show the results of wear tests conducted on the nitrided AISI 316 L, AISI 409 and duplex stainless steels. The tribological properties of the layers obtained were evaluated under conditions of simple metal-metal sliding. The wear rates of the layers changed with the thickness and hardness of the nitrided layers. The presence of the S phase – with high nitrogen content in solid solution and the formation of chrome nitrides – is responsible for the increased wear resistances of the layers.

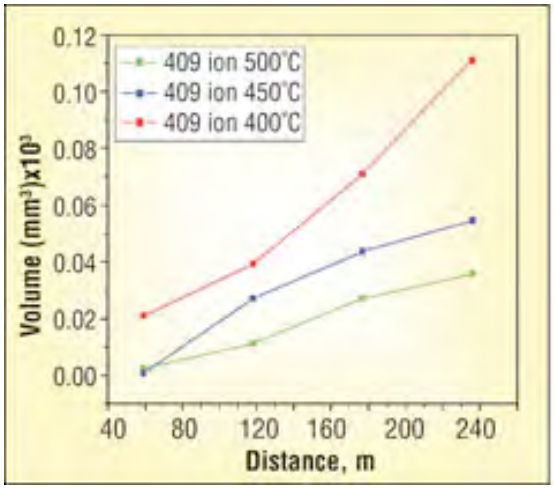


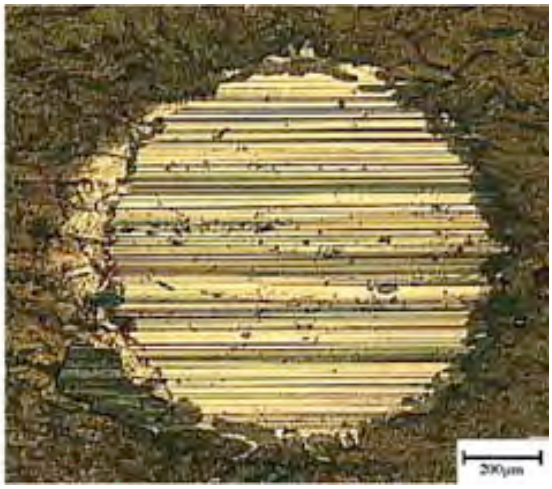


Fig. 16a. Volume loss relative to the sliding distance; Fig. 16b. Cap produced in the AISI 409 sample nitrided at 500□C for 20 minutes

Figures 15b, 16b and 17b show the caps produced in the wear tests. These data show that in all of the cases, the active wear mechanism was the abrasive type characterized by surface scratching. Since the test was performed without the use of abrasives, the scratches were probably produced by hard particles detached from the nitrided layers during the test.

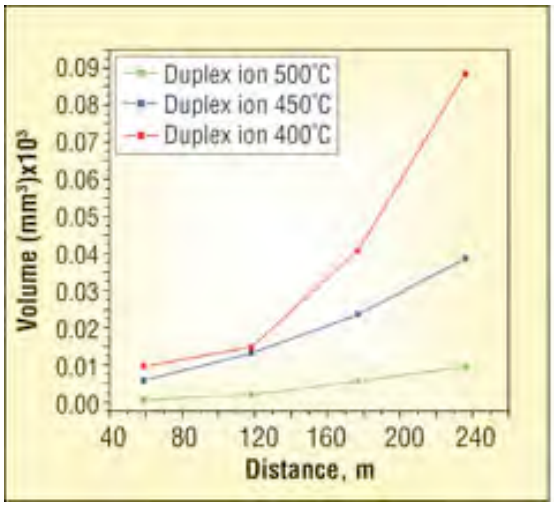



Fig. 17a. Volume loss relative to the sliding distance; Fig. 17b. Cap produced in the duplex sample nitrided at 500□C for 20 minutes

## Corrosion Tests

The corrosion tests were conducted in a 3.5% NaCl aqueous solution with neutral pH. Figures 18, 19 and 20 illustrate the potentiodynamic polarization curves obtained in tests performed on the AISI 316L, AISI 409 and duplex steels in the nitrided and non-nitrided conditions.

For the AISI 316L stainless steel, the sample nitrided at 400□C exhibits the best corrosion resistance with lower passive current density relative to that exhibited by samples nitrided at 450□C and 500□C and the non-nitrided samples.

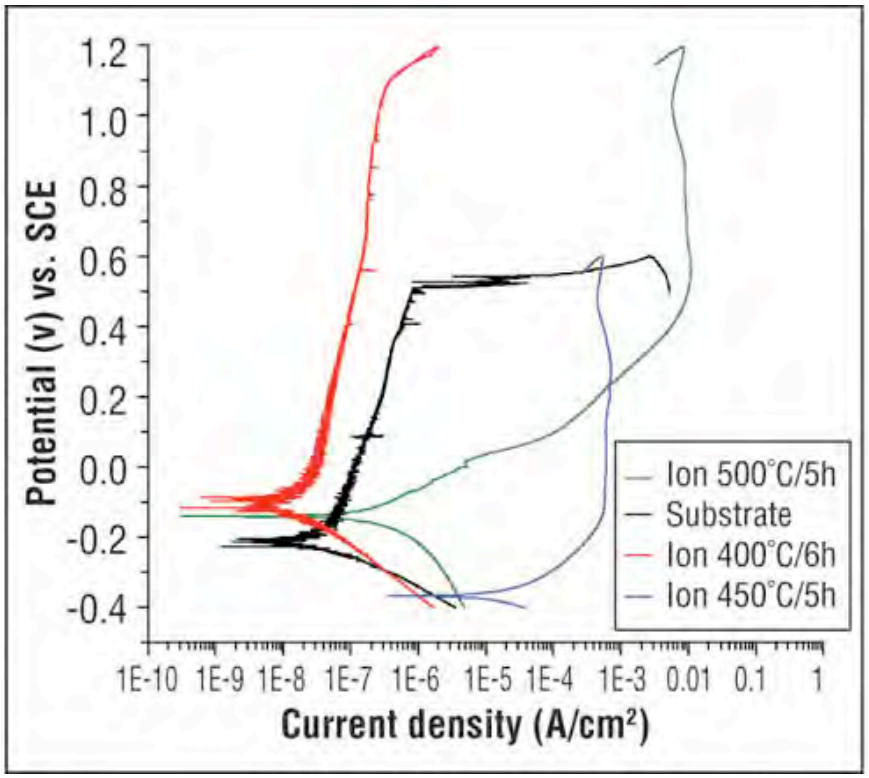


Fig. 18. Potentiodynamic anodic polarization curves for AISI 316L plasma nitrided in the temperatures of 400☒C, 450☒C and 500☒C

For the AISI 409 stainless steel, the samples nitrided at 400☒C and 450☒C provide superior corrosion resistance with a lower passive current density relative to the samples nitrided at 500☒C and the non-nitrided samples. The sample nitrided at 500☒C yielded the poorest corrosion resistance due to the presence of chromium nitride (CrN).

For the duplex stainless steel, the sample nitrided at 400☒C provided the best corrosion resistance with lower passive current density relative to that provided by the samples nitrided at 450☒C and 500☒C and the non-nitrided samples.

Using anodic polarization curves, it is shown that the plasma-nitriding treatments performed at lower temperatures did not reduce the corrosion resistance of the stainless steels. In some cases, an improvement in corrosion resistance by several orders of magnitude compared to base material was observed.

# Conclusions

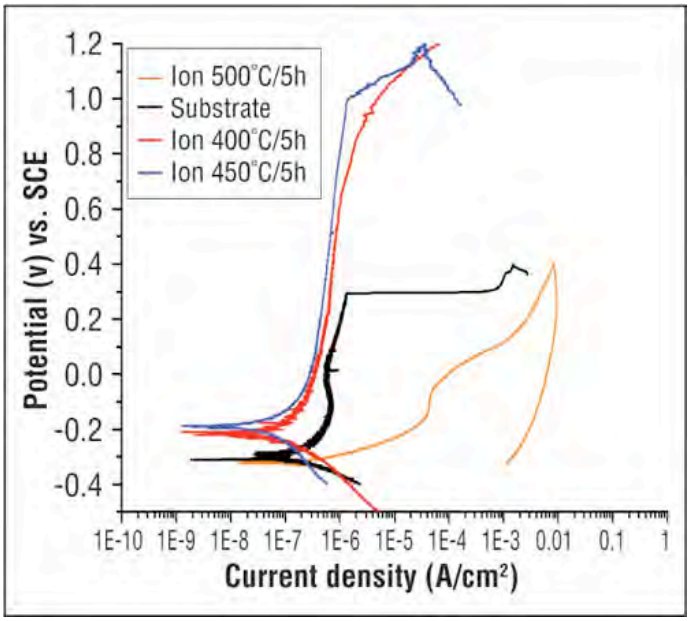


Fig. 19. Potentiodynamic anodic polarization curves for AISI 409 plasma nitrided in the temperatures of 400□C, 450□C and 500□C

**The improvement in the wear resistance of the plasma-nitrided layers shows the effectiveness of the treatments. Improved corrosion resistance of plasma-nitrided layers on stainless steel was also observed when the plasma-nitriding process was conducted at a lower temperature (400□C).**

**The presence of S phase in the nitrided layers, which is characterized by a high nitrogen content in solid solution or chromium nitrides, is responsible for improved performance. Wear resistance of all layers increased with increased layer thickness and treatment temperatures.**

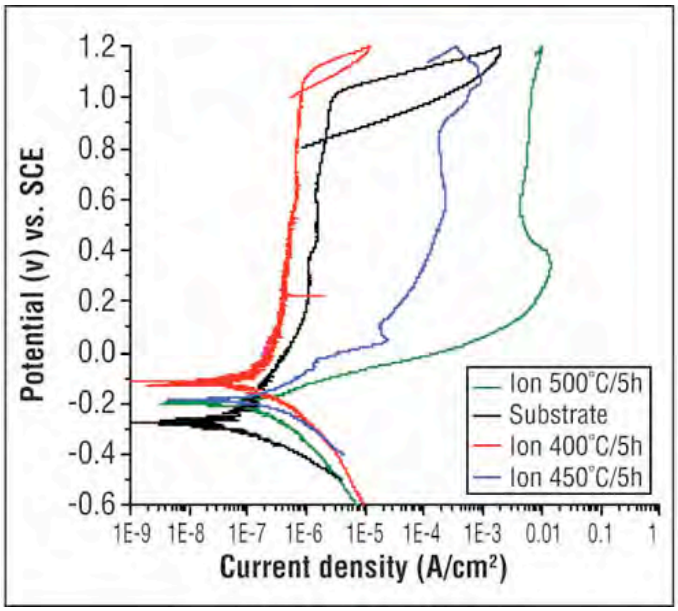


Fig. 20. Potentiodinamic anodic polarization curves for the duplex stainless steel plasma nitrided in the temperatures of 400□C, 450□C and 500□C

## References

1. Handbook of Stainless Steels, Donald Peckner and I.M. Bernstein, McGraw-Hill Book Company, 1977.
2. Metals Handbook, v.4, Heat Treating, American Society for Metals, Metals Park, Ohio, USA, 1991, p. 953-954.
3. Steel Heat Treatment Handbbok, Edited by George E. Totten and Maurice A.H. Howes, Marcl Dekker Inc., 1997, p. 721.
4. Menthe E., Rie K.T., Schultze J.W. and Simson, Surface and Coating Technology, 74-75, 1995, p. 412-416.
5. Sun Y., Bell T., Kolosvary Z. and Flis J., Heat Treatment of Metals, 1999.1, p.9-16.
6. Menthe E. and Rie K.T., Surface and Coating Technology, v. 116-119, 1999, p.199-204.
7. Larisch B., Bruski U. and Spies H.J., Surface and Coating Technology, v. 116-119, 1999, p.205-212.
8. Fewell M.P., Mitchell D.R.G., Priet J.M., Short K.T. and Collins, Surface and Coating Technology, v. 131, 2000, p.300-306.
9. Xu X., Wang l., You Z., Qiang J. and Hei Z., Metallurgical and Materials Transactions A, v. 31A, 2000, p.1193-1199.
10. Xu x., Wang L., Yu z.W.and Hei Z.K., Surface and Coating Technology, v.132, 2000, p. 270-274.
11. Dahm K.L.and Dearnley P. A., Proceedings of the Institution of Mechanical Engeeneers, v.214, part L, 2000, p.181-198.
12. Dearnley P.A., Surface Engineering, v.18, 2002, p.429-432.
13. Bell T., Surface Engineering, v. 18, 2002, p. 415-422.
14. Gontijo L.C., Machado R., Miola E.J., Casteletti L.C., Alcãntara N. G. and Nascente P.A.P., Materials Science & Engineering A, v. 431, 2006, p. 315-321.
15. Gontijo L.C, Machado R., Kuri S.E., Casteletti L.C. and Nascente P.A.P., Thin Solid Films, v.515, 2006, p.1,093-1,096.
16. Pina C.G.F., Dahm K.L., Fisher J. and Dearnley P.A., Wear, v.263, 2007, p. 1,081-1,086.
17. Fontana, M. G. and and Greene N.D.., Corrosion Engineering, McGraw-Hill Int. Book Company,1978, Second Ed., p.321.
**Published with the permission of Industrial Heating Magazine**